Chin. Geogra. Sci. 2021 Vol. 31 No. 2 pp. 197−208
https://doi.org/10.1007/s11769-021-1185-9

Springer Science Press
www.springerlink.com/content/1002-0063

Effect of Hydrological Connectivity on Soil Carbon Storage in the Yellow River Delta Wetlands of China

FENG Jiuge[1], LIANG Jinfeng[1, 2], LI Qianwei[1], ZHANG Xiaoya[1], YUE Yi[1], GAO Junqin[1, 3]

(1. *School of Ecology and Nature Conservation*, *Beijing Forestry University*, *Beijing* 100083, *China*; 2. *State Key Laboratory of Water Environment Simulation*, *School of Environment*, *Beijing Normal University*, *Beijing* 100875, *China*; 3. *The Key Laboratory of Ecological Protection in the Yellow River Basin of National Forestry and Grassland Administration*)

Abstract: Hydrological connectivity has significant effects on the functions of estuarine wetland ecosystem. This study aimed to examine the dynamics of hydrological connectivity and its impact on soil carbon pool in the Yellow River Delta, China. We calculated the hydrological connectivity based on the hydraulic resistance and graph theory, and measured soil total carbon and organic carbon under four different hydrological connectivity gradients (Ⅰ 0–0.03, Ⅱ 0.03–0.06, Ⅲ 0.06–0.12, Ⅳ 0.12–0.39). The results showed that hydrological connectivity increased in the north shore of the Yellow River and the south tidal flat from 2007 to 2018, which concentrated in the mainstream of the Yellow River and the tidal creek. High hydrological connectivity was maintained in the wetland restoration area. The soil total carbon storage and organic carbon storage significantly increased with increasing hydrological connectivity from Ⅰ to Ⅲ gradient and decreased in Ⅳ gradient. The highest soil total carbon storage of 0–30 cm depth was 5172.34 g/m^2, and organic carbon storage 2764.31 g/m^2 in Ⅲ gradient. The hydrological connectivity changed with temporal and spatial change during 2007–2018 and had a noticeable impact on soil carbon storage in the Yellow River Delta. The results indicated that appropriate hydrological connectivity, i.e. 0.08, could effectively promote soil carbon storage.

Keywords: coastal wetland; hydrological connectivity; soil carbon; carbon storage; spatiotemporal variation; the Yellow River Delta

Citation: FENG Jiuge, LIANG Jinfeng, LI Qianwei, ZHANG Xiaoya, YUE Yi, GAO Junqin, 2021. Effect of Hydrological Connectivity on Soil Carbon Storage in the Yellow River Delta Wetlands of China. *Chinese Geographical Science*, 31(2): 197−208. https://doi.org/10.1007/s11769-021-1185-9

1 Introduction

Estuary wetland in river-marine ecotone has important ecological environment effects serving as corridor, filter and barrier (Cao et al., 2018). In recent years, climate change and anthropogenic activities such as reduced freshwater inputs, reclamation, dam construction and over-exploitation have caused wetland shrinking and severe damage to the ecological functions (Deng et al., 2018; Zhang et al., 2018a; Xu et al., 2019).

Studies have shown that the essence of wetlands growth and decline is the destruction of the hydrological cycle with human activities and climate change (Dou et al., 2016; Ala-aho et al., 2018; Higley and Conroy, 2019). The concept of hydrological connectivity has been proposed and evaluated worldwide to describe the process of the hydrological cycle and the relationship between the hydrological and ecological processes (Bracken et al., 2013; Harvey et al., 2019; Liu et al., 2019). The hydrological connectivity refers to the process of transporting water-mediated mass, energy and organisms within or between elements of the hydrolo-

Received date: 2020-03-09; accepted date: 2020-06-22
Foundation item: Under the auspices of the National Key Research and Development Program of China (No. 2017YFC0505903), College Student Research and Career-creation Program of China (No. 201810022070)
Corresponding author: GAO Junqin. E-mail: gaojq@bjfu.edu.cn

gical cycle (Kaller et al., 2015; Thorslund et al., 2018; Conte and Ferro, 2020). Effective hydrological connectivity can preserve the balance of biodiversity, improve water quality, and promote nutrient biogeochemical cycles which especially reflected in enhancing soil carbon storage potential (Karim et al., 2014; Cui et al., 2016a).

Being one of the essential ecological functions of the estuary wetland ecosystem, carbon storage maintains the material circulation and energy flow (Li et al., 2014; Zhang et al., 2016a). Soil organic carbon (SOC) and soil inorganic carbon (SIC) play essential roles in the global carbon cycle, their accumulation and decomposition can directly influence global carbon budget and greenhouse gases (Yu et al., 2013; Zhang et al., 2018b). Studies concluded that soil chemical properties were affected by hydrological connectivity changes during the development of the hydrological process (Bai et al., 2012). Therefore, assessing the relationship between hydrological connectivity and carbon storage function in the estuary wetland ecosystem is crucial to establish a scientific base for restoration and reconstruction of wetlands (Lu and Jiang, 2004). At present, there are many studies on the mechanism and application of the hydrological connectivity around the world (Covino, 2017; Singh and Sinha, 2019). Attention has been given to the evaluation method, spatialtemporal scale assessment, application in habitat restoration and management (Thorslund et al., 2018; Liu et al., 2019). The research on mechanism between hydrological connectivity and the biochemical cycle is on early stage, and the relationship between hydrological connectivity and carbon storage is still unclear (Cui et al., 2016a; Zhang et al., 2019).

The Yellow River Delta is one of the most active regions among the worldwide large river deltas (Zhao et al., 2017). It is the youngest wetland ecosystem in the warm temperate zone of China and plays a significant role in biodiversity conservation and carbon storage (Yu et al., 2016; Zhao et al., 2017). However, owing to climate change and human activities, the hydrological and biological connectivity in estuaries have changed and have even been interrupted in the past recent years (Dou et al., 2016). The Yellow River Delta has been suffering from different degree of degradation, soil salinity and reduction in biodiversity, leading to the recession of the ecosystem structure and function (Song et al., 2018; Cong et al., 2019). With various types of wetland such as tidal creeks and tidal flats, the interaction between freshwater and saltwater is fierce under the double influence of upper reaches and upstream tidal (Cui et al., 2016b; Sun et al., 2020). Driven by natural factors and human activities, the hydrological connectivity in the Yellow River Delta is more complicated and shows a visible change in long-term development (Gao et al., 2017). Researches on soil carbon in the Yellow River Delta are relatively comprehensive, and mainly include the exploration of carbon cycle and mechanism (Lucchese, 2010), the influence of hydrology and vegetation on soil carbon storage (Cao et al., 2013; Zhang et al., 2016b; Schillaci et al., 2017), the estimation methods of carbon storage (Cui et al., 2012). However, little information is available on the response of soil carbon storage function to hydrological connectivity changes over time.

In this study, we calculated the hydrological connectivity from 2007 to 2018 based on the hydraulic resistance and graph theory, and measured soil carbon data in the Yellow River Delta. Specifically, we aimed to: 1) explore how the hydrological connectivity changes in the Yellow River Delta from 2007 to 2018; and 2) examine the relationship between hydrological connectivity and carbon storage in the Yellow River Delta. The results will provide the basis for estuarine wetland restoration and the promotion of carbon storage function.

2 Materials and Methods

2.1 Study area

The study area is located in the Yellow River Delta (37°43′N–37°50′N, 119°03′E–119°13′E), near the south coast of the Bohai Bay and the west coast of the Laizhou Bay (Fig. 1). The Yellow River Delta is one of the most complete, extensive and representative wetland ecosystems in China (Yu et al., 2016). With river changes, upper reaches and erosion of seawater, the Yellow River Delta has become a common interaction area of freshwater and saltwater (Wang et al., 2019a). This region has a warm temperate continental monsoon climate with distinct seasons and contemporary conditions for rain and heat (Zhao et al., 2017). The annual average temperature is 12.1℃, and the annual precipitation is 551.6 mm, 70% of which occurs in July and August. The Yellow River Delta is flat with complex ecological patterns, and its natural slope ranges from 1/8000 to 1/12 000 (Yu et al., 2016). The soil type is

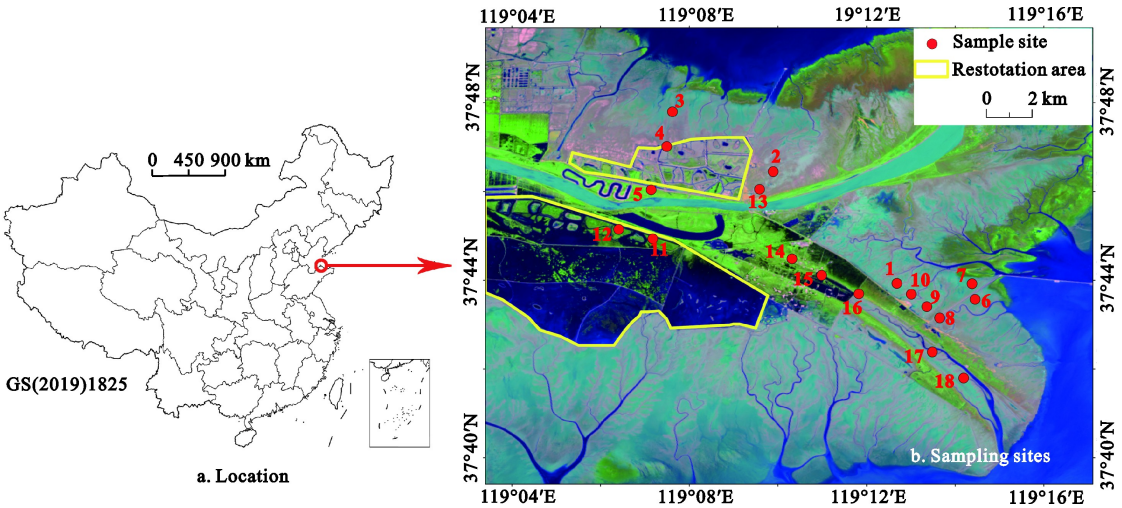

Fig. 1 Location of the Yellow River Delta and sampling sites

mainly saline soil. The dominant species are *Phragmites australis*, *Suaeda glauca* and *Tamarix chinensis* (Bai et al., 2012).

2.2 Hydrological connectivity calculation

According to the historical data of soil carbon and the available data of the river network and channels in the Yellow River Delta in published articles (https://www.cnki.net/), the times and sites of studies were listed in Microsoft Excel 2000. The longitude and latitude of each sampling sites were marked in ArcGIS 10. 2. Based on the study period of these available data, remote sensing images of 2007, 2010, 2015 and 2018 in the Yellow River Delta from Google-Earth with 2.5 m spatial resolution were selected to calculate the hydrological connectivity. Landsat TM/ETM+/OLI (Thematic Mapper/Enhanced Thematic Mapper+/Operational Land Imager) images from the United State Geological Survey (USGS) with 30 m spatial resolution were applied as auxiliary references.

The hydrological connectivity was calculated based on the hydraulic resistance and the graph theory approach, considering the connectivity between the individual sites and the entire network (Xu et al., 2012; Zhu et al., 2017). River network maps in different years were manually interpreted using the spatial analysis method of ArcGIS 10. 2, based on the remote sensing images obtained from Google-earth. Images from USGS were used as auxiliary river identification (Zuecco et al., 2019). Fifty river nodes were chosen to verify the accuracy of river map by field investigation from October 1st to October 7th in 2018. The accuracy of river network maps derived from Google-earth images was over 90%. River channels and tidal creeks could be regarded as edges, and their junctions and sources were considered as nodes (Herrera et al., 2016; Connor-Streich et al., 2018). The river network could be modelled as a mathematical graph (Zhu et al., 2017), $W = (w_{ij})_{p\times p}$, where W is a weighted adjacency matrix; p_i and p_j correspond to nodes, and w_{ij} is the relationship between the adjacent nodes—that is the edge weight. When p_i and p_j are the same node, $w_{ij} = 0$; when p_i and p_j are connected by multiple edges, w_{ij} represents the sum of the edge weights between the two nodes. The edge weights could be calculated based on the flow resistance.

The flow velocity is represented with the Manning formula (Xu et al., 2012):

$$v = \frac{1}{n} R^{\frac{2}{3}} S_f^{\frac{1}{2}} \tag{1}$$

where v is the average flow velocity of the cross-section (m/s), n is the Manning roughness coefficient, R is the hydraulic radius, S_f is the friction slope. In the case of unidirectional flow, S_f can be represented with the channel gradient, and the river flow is determined by the channel gradient or the water head between the nodes. In the case of bidirectional flow, rivers are obstructed by the stream shape and friction (Chen et al., 2016). The Yellow River Delta is flat, which is valid for bidirectional flow. The flow velocity can be written as follows (Xu et al., 2012):

$$v \propto \frac{1}{n} R^{\frac{2}{3}} \tag{2}$$

The hydraulic radius R can be written as (Xu et al., 2012):

$$R = A/X = \frac{(b+mh)h}{b+2h\sqrt{1+m^2}} \quad (3)$$

where A is the longitudinal section area of the channel, X is the wetted perimeter, b is the width measured by the rulers in Google-earth, h is the water depth obtained from existing nautical chart, and m is the slope coefficient. The Manning roughness coefficient and the slope coefficient are obtained by referring to the river design specification and the related studies. Acted by friction, long flowing distance reduces flow velocity (Chen et al., 2016), and the minimal channel gradient in the Yellow River Delta can be ignored. The flow resistance H can be written as:

$$H = \ln\left[\frac{(b+mh)h}{b+2h\sqrt{1+m^2}}\right]^{-\frac{2}{3}} \quad (4)$$

The weighted adjacency matrix is obtained using the inverse of the flow resistance H between adjacent nodes as weight (Xu et al., 2012; Zhu et al., 2017):

$$w_{ij} = \frac{1}{H} \quad (5)$$

The flow fluency matrix $F = (f_{ij})_{n \times n}$ can be established, where f_{ij} is the maximum of the flow fluency between adjacent nodes that is $f_{ij} = \max w_{ij}$. The flow fluency D_i of any node is represented with the average of f_{ij}. The weighted hydrological connectivity D of one sample can average D_i of the surrounding nodes:

$$D_i = \frac{1}{n+1}\sum_{i=1}^{n}\sum_{j=1}^{n} f_{ij} \quad (6)$$

$$D = \frac{1}{n}\sum_{i=1}^{n} D_i, i = 1,2,\cdots,n \quad (7)$$

According to the flow fluency D_i, the spline interpolation method was used to express the distribution of the hydrological connectivity in the Yellow River Delta, and the gradients were performed by the natural breaks method (Wang et al., 2019b). Four hydrological connectivity gradients were determined, namely: Ⅰ (0–0.03), Ⅱ (0.03–0.06), Ⅲ (0.06–0.12) and Ⅳ (0.12–0.39).

2.3 Sample collection and analysis

A total of 18 plots were chosen based on the literature and the calculation results of the hydrological connectivity, including the typical plots under different hydrological connectivity gradients and the plots with significant changes in hydrological connectivity during 2007–2018 (Appendix Table 1). Soil carbon data of 18 plots during 2007–2015 was extracted from literature and the data of 2018 was measured. In 2018, soil samples with four replicates were collected at each depth of 0–10, 10–20, 20–30 cm at each plot in July and October 2018. There were in total 216 samples. Plant species were investigated at the same time. The plant coverage of Ⅰ (0–0.03) was 25%, Ⅱ (0.03–0.06) 45%, Ⅲ (0.06–0.12) 62%, and Ⅳ (0.12–0.39) 91%. The dominant species in the Yellow River Delta were *P. australis*, *S. glauca* and *T. chinensis*. *P. australis* was widely distributed in the four gradients, while *S. glauca* and *T. chinensis* were not recorded in Ⅳ (0.12–0.39) gradient. As the hydrological connectivity increases, typical species such as *Triarrhena lutarioriparia*, *Scirpus validu* appeared in the plots, as well as vines and woody plants (e.g., *Humulus scandens*, *Sophora japonica*).

The soil samples were placed in polyethene bags, kept on ice and stored in the laboratory until subsequent processing. One part of the soil samples was air-dried at room temperature for three weeks, while another part was kept in cold storage. Plant litters, roots and the stone were removed before analysis. After pre-treatment, two samples of 100 mg soil with and without 10% hydrochloric acid were dried at 105℃ for at least 4.0 h, and measured for SOC and TC by Multi N/C 3100 analyzer. Five gram soil sample with distilled water was extracted for 1.5 h and then filtered to measure dissolved organic carbon (DOC) using Multi N/C 3100 analyzer. The soil inorganic carbon (TIC) is TC minus TOC. The physical properties (soil bulk density and moisture content) were measured at the same time.

Soil carbon storage at certain layers of each sampling site was calculated by the following equation (Zhao et al., 2016):

$$TCS = BD_i \times TC_i \times h \quad (8)$$

$$SOCS = BD_i \times SOC_i \times h \quad (9)$$

where TCS is the carbon storage (g/m^2), $SOCS$ is the organic carbon storage (g/m^2), BD_i is the soil bulk density of soil layer i (g/cm^3), h is the layer thickness (m), TC_i and SOC_i are TC and SOC contents of the soil layer i (mg/kg).

2.4 Statistical analyses and graphing

Repeated measures analysis of variance (ANOVA) was used to test the effects of soil depth and hydrological connectivity on soil carbon storage. Linear regression

analysis was performed to identify the relationship between TCS, SOCS and the hydrological connectivity. The differences were considered significant when $P < 0.05$. Statistical analyses were carried out using SPSS 20.0 software package. The graphs were created with Sigmaplot 12.5 package.

3 Results

3.1 The change of hydrological connectivity

The pattern of hydrological connectivity in the Yellow River Delta showed an increasing trend from margin to centre during 2007–2018 (Fig. 2). In 2007, high hydrological connectivity concentrated in the wetland restoration area in south shore of the Yellow River and was maintained for long-term. Since 2010, the north shore where rivers were dense reached Ⅳ (0.12–0.39) gradient, and many high hydrological connectivity centres scattered in the nouth shore. In 2015, high hydrological connectivity areas showed a connecting trend and extended to the Old Yellow River. In 2018, high hydrological connectivity areas widely distributed in the north shore of the Yellow River and the south tidal flats, concentrating in both sides of the Yellow River and the tidal creeks. Hydrological connectivity in the South shore decreased, but the value remained relatively high (Ⅳ 0.12–0.39).

The proportion of high hydrological connectivity areas in the Yellow River Delta increased gradually during 2007–2018 (Fig. 3). The proportion of low hydrological connectivity area (Ⅰ 0–0.03) was the highest during 2007–2018, and decreased obviously since 2010, from 69.92% to 53.73% in 2018. The proportion of Ⅱ (0.03–0.06) and Ⅲ (0.06–0.12) gradient increased signi-

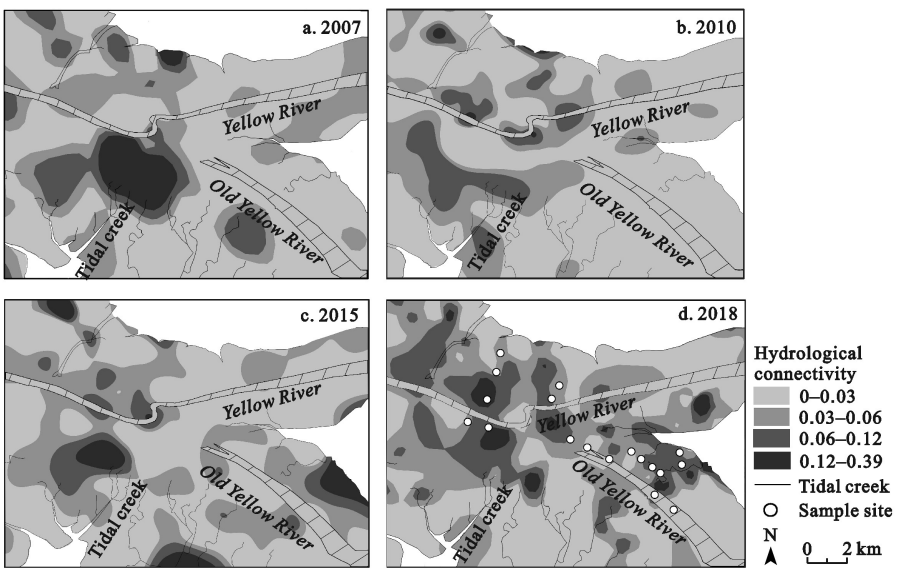

Fig. 2 Hydrological connectivity of the Yellow River Delta in 2007, 2010, 2015 and 2018

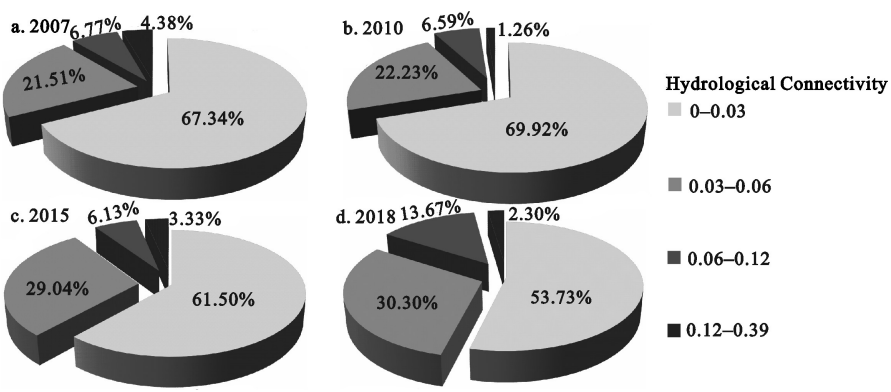

Fig. 3 The area percentages of different hydrological connectivity gradients in the Yellow River Delta in 2007 (a), 2010 (b), 2015 (c), 2018 (d)

ficantly, and the highest values were 30.30% and 13.67%, respectively in 2018, increasing by 8.79% and 7.54% compared with those in 2007. The proportion of high hydrological connectivity area (Ⅳ 0.12–0.39) was the lowest during 2007–2018 and exhibited no noticeable change.

3.2 Soil carbon storage with different hydrological connectivity

3.2.1 Soil carbon content with different hydrological connectivity

Hydrological connectivity had significant effects on TC, SOC and DOC in 2018 ($P < 0.001$; Table 1). With increasing hydrological connectivity, TC, SOC and TIC contents firstly increased, then subsequently decreased (Fig. 4). The peak average content of TC was 11.64–12.90 g/kg, and SOC 5.02–6.60 g/kg in Ⅲ (0.06–0.12) gradient. The average contents of TC and SOC decreased in Ⅳ (0.12–0.39) gradient, which were 8.30–10.31 g/kg and 2.99–4.89 g/kg, respectively. TIC showed a consistent tendency with TC and SOC while exhibited no significant difference in the four gradients ($P > 0.05$). DOC content was significantly higher in Ⅰ (0–0.03) gradient, which was 491.49–509.62 mg/kg, showing a different trend compared to TC, SOC and TIC. SOC, TIC and DOC showed no significant differences with the variation of depths ($P > 0.05$). The upper soil (0–10 cm) had higher contents of TC than the deeper layer (10–20 cm) in Ⅳ (0.12–0.39) gradient. There was an interaction effect between the hydrological connectivity and

Table 1 Effects of hydrological connectivity on soil total carbon (TC), organic carbon (SOC), inorganic carbon (TIC) and dissolved organic carbon (DOC) content at different depths in the Yellow River Delta

Parameter	Hydrological connectivity		Depths		Hydrological connectivity × Depths	
	F	*P*	*F*	*P*	*F*	*P*
TC	**10.88**	0.000***	**3.30**	0.040*	1.73	0.118
SOC	**16.36**	0.000***	2.66	0.074	**2.28**	0.039*
TIC	2.62	0.058	0.34	0.712	1.19	0.315
DOC	**21.50**	0.000***	0.15	0.858	1.82	0.103

Notes: The given are *F* and *P* of ANOVA. * $P < 0.05$, ** $P < 0.01$, *** $P < 0.001$. the *F* values with $P < 0.05$ are in bold

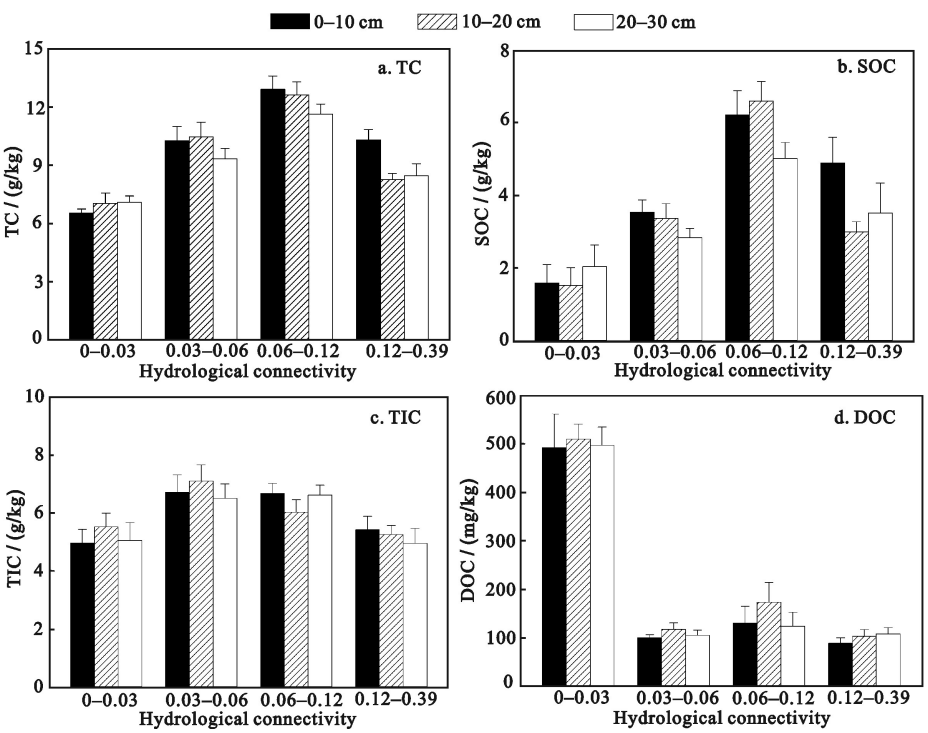

Fig. 4 The contents of total carbon (TC), organic carbon (SOC), total inorganic carbon (TIC) and dissolved organic carbon (DOC) in different hydrological connectivity gradients in the Yellow River Delta in 2018

soil depths on SOC, but not on TC, TIC and DOC.

3.2.2 Soil carbon storage with different hydrological connectivity

With increasing hydrological connectivity, TCS and SOCS firstly increased, and subsequently decreased (Fig. 5). The peak of TCS and SOCS in 0–30 cm layer were 5172.34 g/m^2 and 2764.31 g/m^2 respectively in III (0.06–0.12) gradient. The lowest TCS and SOCS in 0–30 cm layer were 3184.77 g/m^2 and 694.19 g/m^2 respectively in I (0–0.03) gradient.

There was a noticeable non-linear relationship between the hydrological connectivity and carbon storage in the spatial and temporal distribution (Figs. 6 and 7). When the hydrological connectivity was below 0.08, there was a significant positive correlation between TCS and hydrological connectivity, as well as between SOCS and hydrological connectivity ($P < 0.001$, Fig. 6). When the hydrological connectivity was around 0.08, TCS and SOCS reached the peak (Fig. 6). There was a significant negative correlation between TCS and hydrological connectivity, as well as between SOCS and hydrological connectivity when the hydrological connectivity was above 0.08 ($P < 0.001$, Fig. 6). The temporal change showed a consistent trend with spatial characteristics (Fig. 7).

4 Discussion

4.1 Hydrological connectivity

Our results showed that high hydrological connectivity concentrated in the mainstream of the Yellow River and tidal creeks during 2007–2018. South wetland restoration area has kept high hydrological connectivity for the long-term. This implied hydrological connectivity was closely related to the river distribution and the number of nodes. Water patches were centralised in the south shore of the Yellow River but scattered in other areas. So the number of nodes was fewer, and the average number of rivers connected by nodes was more substan-

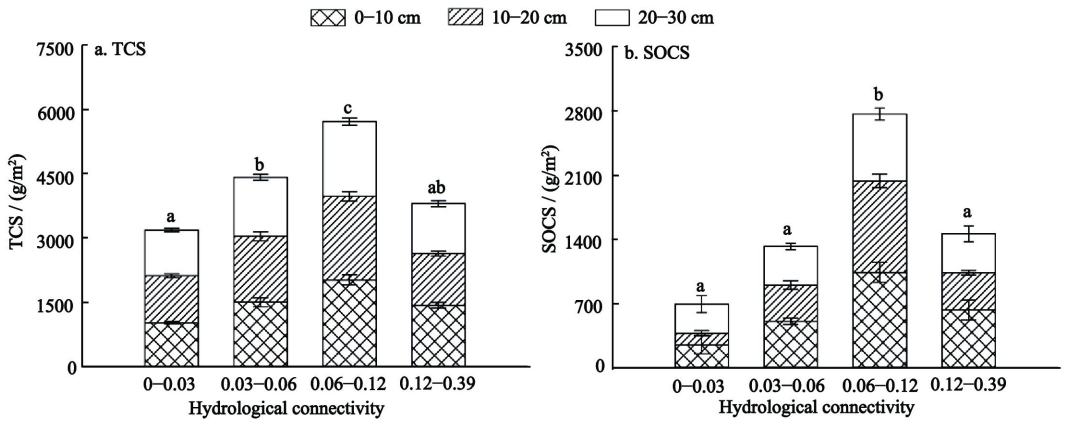

Fig. 5 Total carbon storage (TCS) and organic carbon storage (SOCS) in different hydrological connectivity gradients in the Yellow River Delta in 2018. Different lowercase letters indicate significant differences among the whole columns in different hydrological connectivity gradients ($P < 0.05$)

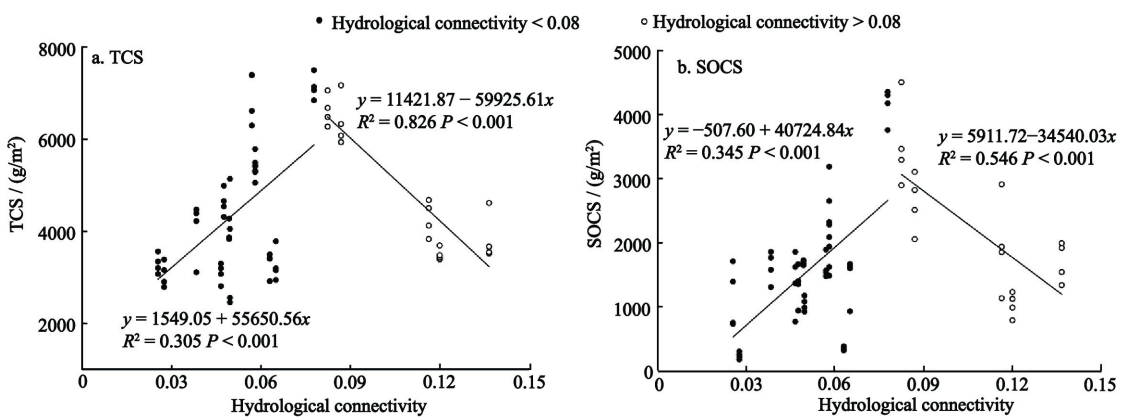

Fig. 6 Relationship between hydrological connectivity and total soil carbon storage (TCS), organic carbon storage (SOCS) in the Yellow River Delta in 2018

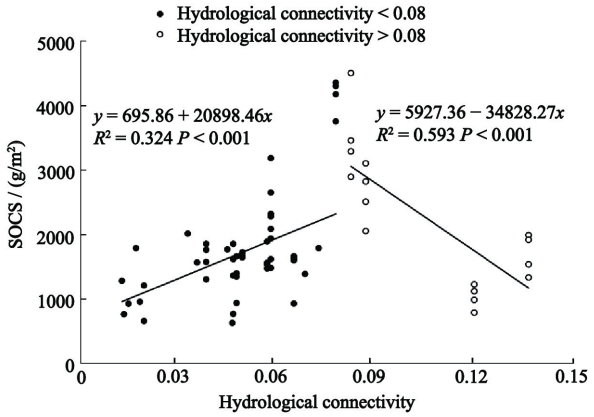

Fig. 7 Relationship between hydrological connectivity and organic carbon storage (SOCS) during 2007–2018 in the Yellow River Delta

tial in the south shore, maintaining high hydrological connectivity for long-term. This was consistent with previous results (Yu et al., 2019; Wang et al., 2019a). The results showed that the hydrological connectivity in the north tidal flat was always higher than that in the South. This was because more loop connection in the north shaped more complicated river network (Yu et al., 2019). The deltas worldwide showed same features on their forked river nets (Tejedor et al., 2015; Herrera et al., 2016). Sedimentation and fork control the fractal dimension of delta river network, which is about 1.2–1.3 (Edmonds et al., 2011). More complicated forked rivers could have more loops, leading to higher hydrology connectivity (Liu et al., 2019). Besides, tidal plays an important role in deltas. Researches in the Ganges Delta and Wax Lake Delta showed that tidal-affected area had higher hydrological connectivity (Passalacqua et al., 2013; Hiatt and Passalacqua, 2015). Tidal flow restoration could improve the inputs and accumulation of soil organic matter, which could be a measure to enhance hydrological connectivity and soil carbon storage (Gao et al., 2014; Zhao et al., 2018; Wang et al., 2019a).

Apart from natural factors, human activities such as water-sediment regulation projects also have essential impacts on natural hydrological connectivity (Deng et al., 2018). Diversion channels were built to replenish freshwater in both the north and south shores. However, there were embankments at every 600 m to retain and distribute water in the north shore, thereby blocking hydrological connectivity (Wang et al., 2011). The south shore is in the core area of the Yellow River Delta, so there was little human disturbance. The large area of surface water formed closed flow paths with the mainstream of the Yellow River, contributing to high hydrological connectivity (Guo et al., 2019). Meanwhile, water-sediment regulation contributed to the increase of the third-level tidal creeks. This promoted a linear connection and enhanced the overall hydrological connectivity (Wang et al., 2019a; Yu et al., 2019). Research showed that deltas had self-organized ability to settle species and deal with climate change, so the Ⅰ and Ⅳ gradients had little increasing degree to avoid negative impacts (Edmonds et al., 2011; Liu et al., 2019).

4.2 Effect of hydrological connectivity on soil carbon storage

With increasing hydrological connectivity, TC and SOC firstly increased from Ⅰ (0–0.03) gradient to Ⅲ (0.06–0.12) gradient and then decreased in Ⅳ (0.12–0.39) gradient. TCS and SOCS exhibited very similar trends. This might be due to the change in plant coverage and species. Appropriate hydrological connectivity could increase the plant species richness, coverage as well as the productivity, and finally promoted organic matter accumulation (Bai et al., 2016; Zhang et al., 2019). At the same time, *S. glauca* existed in Ⅰ, Ⅱ and III gradients, but not in Ⅳ gradient. Compared with other species, *S. glauca* can quickly wither and return to the soil to supply the organic matter. This finding agrees with the result reported in Jia et al. (2015). DOC was significantly lower in high hydrological connectivity than in low hydrological connectivity. This may be because the soluble soil materials mostly transferred into water and were taken away (Osburn et al., 2017; Senar et al., 2018).

Previous researches showed that the increase of the hydrological connectivity could affect water, plants, soils, etc. to promote the circulation of the nutrients (Means et al., 2016; Reid et al., 2016; Xia et al., 2017). Hydrological connectivity controlled the existence pattern of plant and was conversely supported by plant diversity through microtopographic variation (Cui et al., 2016a). The results showed that plant coverage was positively related to hydrological connectivity, which was consistent with previous studies (Liu et al., 2020). Besides, a previous study showed that perennial species could effectively accumulate carbon over time because of their biomass storage ability (Means et al., 2016). This means that the co-work of hydrological connectivity and plant diversity could enhance the soil carbon storage capacity (Xia et al., 2017; Zhang et al., 2019).

4.3 Relationship between hydrological connectivity and soil carbon storage

Our results showed that the soil carbon storage was the highest when the hydrological connectivity was 0.08, whether in temporal or spatial scale. This indicated that the appropriate hydrological connectivity could promote organic matter input and enhance the circulation of nutrients in wetlands (Bai et al., 2012; Zhao et al., 2016). Water conservancy projects such as dams could hinder the longitudinal water flow and sediment transport (Winemiller et al., 2016). This could lead to low hydrological connectivity and reduce the natural capacity of nutrient retain (Covino et al., 2012; Covino, 2017). Conversely, ditches could boost the connection of flow and lead to high hydrological connectivity (Schmidt and Wilcock, 2008). High hydrological connectivity could reduce retention time of flow and make nutrients difficult to retain (Osburn et al., 2017; Senar et al., 2018). Natural rivers are in between. Due to human activities and climate change, the natural state of wetland could change and affect nutrients retention capacity (Covino et al., 2017). In this research, when hydrological connectivity was exceeded 0.08, it could drive soil dissolved materials into water and perhaps hinder soil carbon storage (Osburn et al., 2017; Senar et al., 2018). Previous studies showed that appropriate hydrological connectivity could contribute to high carbon input and accumulation rate (Suir et al., 2019). Excessive hydrological connectivity could deteriorate the ecological function and habitat stability (Myers and Harms, 2009; Dou et al., 2016). Although our results reflected the spatial pattern between hydrological connectivity and soil carbon storage, it can be further expanded of the sites and samples for further investigation, and the mechanisms are still worth exploring.

5 Conclusions

The results showed that hydrological connectivity significantly changed with temporal and spatial change during 2007–2018, and thereby had an impact on soil carbon pool in the Yellow River Delta. High hydrological connectivity concentrated in the mainstream of the Yellow River and tidal creeks during 2007–2018. The soil total carbon storage and organic carbon storage significantly increased with increasing hydrological connectivity from 0 to 0.12 and decreased in 0.12–0.39. Suitable hydrological connectivity, i.e., 0.08, could promote soil carbon storage effectively in temporal and spatial scale. Further studies are still needed to examine the influencing mechanisms of the hydrological connectivity on the soil carbon storage in the Yellow River Delta, especially with regards to the long-term and seasonal effects to propose a scientific base for estuary wetland restoration.

Appendix

Table 1 The information of sources and locations about the 18 plots used in this study

Number	Longitude	Latitude	References	Flooding condition	Human activities	Land type	Vegetations
1	119°12′36″E	37°43′48″N	Xia et al., 2015	Tidal flooding	None	Tidal flat	Reed salty swamp
2	119°9′36″E	37°46′12″N	Yu et al., 2010	Seasonal flooding	None	Salt marsh	*Suaeda* community
3	119°7′48″E	37°47′24″N	Luo et al., 2010	Tidal flooding	None	Tidal flat	Bare land
4	119°7′12″E	37°46′48″N	Luo et al., 2010	Long term flooding	None	Clear water	Water
5	119°7′12″E	37°46′12″N	Luo et al., 2010	Seasonal flooding	Traffic impact	Grass land	Reed meadow
6	119°14′24″E	37°43′12″N	Jia et al., 2015	Tidal flooding	None	Tidal flat	*Suaeda* community
7	119°14′24″E	37°43′48″N	Jia et al., 2015	Tidal flooding	None	Tidal flat	Reed salty swamp
8	119°13′48″E	37°43′12″N	Jia et al., 2015	Tidal flooding	None	Tidal flat	Reed salty swamp
9	119°13′12″E	37°43′12″N	Jia et al., 2015	Tidal flooding	None	Tidal flat	Reed salty swamp
10	119°12′36″E	37°43′12″N	Jia et al., 2015	Tidal flooding	None	Tidal flat	Reed salty swamp
11	119°7′12″E	37°45′00″N	Yin, 2011	Seasonal flooding	Traffic impact	Grass land	Reed meadow
12	119°6′36″E	37°45′00″N	Yin, 2011	Seasonal flooding	Traffic impact	Grass land	Reed meadow
13	119°10′12″E	37°46′12″N	Yin, 2011	Seasonal flooding	None	Tidal flat	*Tamarix* community
14	119°10′12″E	37°44′24″N	Zou et al., 2015	Seasonal flooding	None	Grass land	Reed meadow
15	119°10′48″E	37°44′24″N	Zou et al., 2015	Seasonal flooding	None	Built up	Reed meadow
16	119°12′00″E	37°43′48″N	Zou et al., 2015	Seasonal flooding	Oil operation	Grass land	Reed meadow
17	119°13′48″E	37°42′00″N	Zou et al., 2015	Tidal flooding	Oil operation	Tidal flat	*Suaeda* community
18	119°14′24″E	37°42′00″N	Zou et al., 2015	Tidal flooding	Oil operation	Tidal flat	*Suaeda* community

References

Ala-aho P, Soulsby C, Pokrovsky O S et al., 2018. Using stable isotopes to assess surface water source dynamics and hydrological connectivity in a high-latitude wetland and permafrost influenced landscape. *Journal of Hydrology*, 556: 279–293. doi: 10.1016/j.jhydrol.2017.11.024

Bai J H, Wang J J, Yan D H et al., 2012. Spatial and temporal distributions of soil organic carbon and total nitrogen in two marsh wetlands with different flooding frequencies of the Yellow River Delta, China. *Clean-Soil Air Water*, 40(10): 1137–1144. doi: 10.1002/clen.201200059

Bai J H, Zhang G L, Zhao Q Q et al., 2016. Depth-distribution patterns and control of soil organic carbon in coastal salt marshes with different plant covers. *Scientific Reports*, 6(1): 34835. doi: 10.1038/srep34835

Bracken L J, Wainwright J, Ali G A et al., 2013. Concepts of hydrological connectivity: research approaches, pathways and future agendas. *Earth-Science Reviews*, 119: 17–34. doi: 10.1016/j.earscirev.2013.02.001

Cao Lei, Song Jinming, Li Xuegang et al., 2013. Research progresses in carbon budget and carbon cycle of the coastal salt marshes in China. *Acta Ecologica Sinica*, 33(17): 5141–5152. (in Chinese)

Cao Zihao, Zhao Qinghe, Zuo Xianyu et al., 2018. Optimizing vegetation pattern for the riparian buffer zone along the lower yellow river based on slope hydrological connectivity. *Chinese Journal of Applied Ecology*, 29(3): 739–747. (in Chinese)

Chen Xing, Xu Wei, Li Kunpeng et al., 2016. Evaluation of plain river network connectivity based on graph theory: a case study of Yanjingwei in Changshu city. *Water Resources Protection*, 32(2): 26–29, 34. (in Chinese)

Connor-Streich G, Henshaw A J, Brasington J et al., 2018. Let's get connected: a new graph theory-based approach and toolbox for understanding braided river morphodynamics. *WIREs Water*, 5(5): e1296. doi: 10.1002/wat2.1296

Conte P, Ferro V, 2020. Standardizing the use of fast-field cycling NMR relaxometry for measuring hydrological connectivity inside the soil. *Magnetic Resonance in Chemistry*, 58(1): 41–50. doi: 10.1002/mrc.4907

Covino T, McGlynn B, McNamara R, 2012. Land use/land cover and scale influences on in-stream nitrogen uptake kinetics. *Journal of Geophysical Research*, 117(G2): G02006. doi: 10.1029/2011JG001874

Covino T, 2017. Hydrologic connectivity as a framework for understanding biogeochemical flux through watersheds and along fluvial networks. *Geomorphology*, 277: 133–144. doi: 10.1016/j.geomorph.2016.09.030

Cui Baoshan, Cai Yanzi, Xie Tian et al., 2016a. Ecological effects of wetland hydrological connectivity: problems and prospects. *Journal of Beijing Normal University (Natural Science)*, 52(6): 738–746. (in Chinese)

Cui Lijuan, Ma Qiongfang, Song Hongtao et al., 2012. Estimation methods of wetland ecosystem carbon storage: a review. *Chinese Journal of Ecology*, 31(10): 2673–2680. (in Chinese)

Cui Zhen, Shen Hong, Zhang Guangxin, 2016b. Changes of landscape patterns and hydrological connectivity of wetlands in Momoge National Natural Wetland Reserve and their driving factors for three periods. *Wetland Science*, 14(6): 866–873. (in Chinese)

Deng X J, Xu Y P, Han L F, 2018. Impacts of human activities on the structural and functional connectivity of a river network in the Taihu Plain. *Land Degradation & Development*, 29(8): 2575–2588. doi: 10.1002/ldr.3008

Dou P, Cui B S, Xie T et al., 2016. Macrobenthos diversity response to hydrological connectivity gradient. *Wetlands*, 36(1): 45–55. doi: 10.1007/s13157-014-0580-8

Edmonds D A, Paola C, Hoyal D C J D et al., 2011. Quantitative metrics that describe river deltas and their channel networks. *Journal of Geophysical Research*, 116(F4): F04022. doi: 10.1029/2010JF001955

Gao Changjun, Gao Xiaocui, Jia Peng, 2017. Summary comments on hydrologic connectivity. *Chinese Journal of Applied & Environmental Biology*, 23(3): 586–594. (in Chinese)

Gao M S, Liu S, Zhao G M et al., 2014. Vulnerability of eco-hydrological environment in the Yellow River Delta Wetland. *Journal of Coastal Research*, 30(2): 344–350. doi: 10.2112/JCOASTRES-D-13-00016.1

Guo Yutong, Cui Yuan, Wang Chen et al., 2019. Distribution characteristics of carbon and nitrogen stable isotopes in wetland components and their relationship with wetland hydrological connectivity. *Journal of Nature Resources*, 34(12): 2554–2568. (in Chinese)

Harvey J, Gomez-Velez J, Schmadel N et al., 2019. How hydrologic connectivity regulates water quality in river corridors. *Journal of the American Water Resources Association*, 55(2): 369–381. doi: 10.1111/1752-1688.12691

Herrera M, Abraham E, Stoianov I, 2016. A graph-theoretic framework for assessing the resilience of sectorised water distribution networks. *Water Resources Management*, 30(5): 1685–1699. doi: 10.1007/s11269-016-1245-6

Hiatt M, Passalacqua P, 2015. Hydrological connectivity in river deltas: the first-order importance of channel-island exchange. *Water Resources Research*, 51(4): 2264–2282. doi: 10.1002/2014WR016149

Higley M C, Conroy J L, 2019. The hydrological response of surface water to recent climate variability: a remote sensing case study from the central tropical Pacific. *Hydrological Processes*, 33(16): 2227–2239. doi: 10.1002/hyp.13465

Jia Jia, Bai Junhong, Gao Zhaoqin et al., 2015. Carbon and nitrogen contents and storages in the soils of intertidal salt marshes in the Yellow River Delta. *Wetland Science*, 13(6): 714–721. (in Chinese)

Kaller M D, Keim R F, Edwards B L et al., 2015. Aquatic vegetation mediates the relationship between hydrologic connectivity and water quality in a managed floodplain. *Hydrobiologia*, 760(1): 29–41. doi: 10.1007/s10750-015-2300-7

Karim F, Kinsey-Henderson A, Wallace J et al., 2014. Modelling hydrological connectivity of tropical floodplain wetlands via a combined natural and artificial stream network. *Hydrological Processes*, 28(23): 5696–5710. doi: 10.1002/hyp.10065

Li Yuan, Zhang Haibo, Chen Xiaobing et al., 2014. Gradient distributions of nitrogen and organic carbon in the soils from inland to tidal flat in the Yellow River Delta. *Geochimica*, 43(4): 338–345. (in Chinese)

Liu J K, Engel B A, Wang Y et al., 2019. Runoff response to soil moisture and micro-topographic structure on the plot scale. *Scientific Reports*, 9(1): 2532. doi: 10.1038/s41598-019-39409-6

Liu J K, Engel B A, Wang Y et al., 2020. Multi-scale analysis of hydrological connectivity and plant response in the Yellow River Delta. *Science of the Total Environment*, 702: 134889. doi: 10.1016/j.scitotenv.2019.134889

Lu Xianguo, Jiang Ming, 2004. Progress and prospect of wetland research in China. *Journal of Geographical Sciences*, 14(1): 45–51. doi: 10.1007/bf02841106

Lucchese M, Waddington J M, Poulin M et al., 2010. Organic matter accumulation in a restored peatland: evaluating restoration success. *Ecological Engineering*, 36(4): 482–488. doi: 10.1016/j.ecoleng.2009.11.017

Luo Xianxiang, Yan Qin, Yang Jianqiang et al., 2010. Study on seasonal variation characteristics and transformation process of soil nitrogen in Yellow River estuary wetland. *Journal of Soil and Water Conservation*, 24(6): 88–93. (in Chinese)

Means M M, Ahn C, Korol A R et al., 2016. Carbon storage potential by four macrophytes as affected by planting diversity in a created wetland. *Journal of Environmental Management*, 165: 133–139. doi: 10.1016/j.jenvman.2015.09.016

Myers J A, Harms K E, 2009. Seed arrival, ecological filters, and plant species richness: a meta-analysis. *Ecology Letters*, 12(11): 1250–1260. doi: 10.1111/j.1461-0248.2009.01373.x

Osburn C L, Anderson N J, Stedmon C A et al., 2017. Shifts in the source and composition of dissolved organic matter in Southwest Greenland lakes along a regional hydro-climatic gradient. *Journal of Geophysical Research*, 122(12): 3431–3445. doi: 10.1002/2017JG003999

Passalacqua P, Lanzoni S, Paola C et al., 2013. Geomorphic signatures of deltaic processes and vegetation: the Ganges-Brahmaputra-Jamuna case study. *Journal of Geophysical Research*, 118(3): 1838–1849. doi: 10.1002/jgrf.20128

Reid M A, Reid M C, Thoms M C, 2016. Ecological significance of hydrological connectivity for wetland plant communities on a dryland floodplain river, Macintyre River, Australia. *Aquatic Science*, 78(1): 139–158. doi: 10.1007/s00027-015-0414-7

Schillaci C, Acutis M, Lombardo L et al., 2017. Spatio-temporal topsoil organic carbon mapping of a semi-arid Mediterranean region: the role of land use, soil texture, topographic indices and the influence of remote sensing data to modelling. *Science of the Total Environment*, 601–602: 821–832. doi: 10.1016/j.scitotenv.2017.05.239

Schmidt J C, Wilcock P R, 2008. Metrics for assessing the downstream effects of dams. *Water Resources Research*, 44(4): W04404. doi: 10.1029/2006wr005092

Senar O E, Webster K L, Creed I F, 2018. Catchment-scale shifts in the magnitude and partitioning of carbon export in response to changing hydrologic connectivity in a northern hardwood forest. *Journal of Geophysical Research*, 123(8): 2337–2352. doi: 10.1029/2018JG004468

Singh M, Sinha R, 2019. Evaluating dynamic hydrological connectivity of a floodplain wetland in North Bihar, India using geostatistical methods. *Science of the Total Environment*, 651: 2473–2488. doi: 10.1016/j.scitotenv.2018.10.139

Song Hongli, Liu Xingtu, Wang Lizhi et al., 2018. Spatial and temporal distribution of soil organic carbon in vegetation communities of the Yellow River Delta under different disturbance levels. *Journal of Soil and Water Conservation*, 32(1): 190–196, 203. (in Chinese)

Suir G M, Sasser C E, DeLaune R D et al., 2019. Comparing carbon accumulation in restored and natural wetland soils of coastal Louisiana. *International Journal of Sediment Research*, 34(6): 600–607. doi: 10.1016/j.ijsrc.2019.05.001

Sun Jingkuan, Chi Yuan, Fu Zhanyong et al., 2020. Spatiotemporal variation of plant diversity under a unique estuarine wetland gradient system in the Yellow River Delta, China. *Chinese Geographical Science*, 30(2): 217–232. doi: 10.1007/s11769-020-1109-0

Tejedor A, Longjas A, Zaliapin I et al., 2015. Delta channel networks: 1. A graph-theoretic approach for studying connectivity and steady state transport on deltaic surfaces. *Water Resources Research*, 51(6): 3998–4018. doi: 10.1002/2014WR016577

Thorslund J, Cohen M J, Jawitz J W et al., 2018. Solute evidence for hydrological connectivity of geographically isolated wetlands. *Land Degradation & Development*, 29(11): 3954–3962. doi: 10.1002/ldr.3145

Wang H, Wang R Q, Yu Y et al., 2011. Soil organic carbon of degraded wetlands treated with freshwater in the Yellow River Delta, China. *Journal of Environmental Management*, 92(10): 2628–2633. doi: 10.1016/j.jenvman.2011.05.030

Wang Jianbu, Zhang Jie, Ma Yi et al., 2019a. Estimation of vegetation carbon storage in the Yellow River estuary wetland based on GF-1 WFV satellite image. *Advances in Marine Science*, 37(1): 75–83. (in Chinese)

Wang Qian, Cui Yuan, Wang Chen et al., 2019b. Screening of priority restoration nodes in wetlands in Yellow River Delta based on plankton community and hydrological connectivity. *Wetland Science*, 17(3): 324–334. (in Chinese)

Winemiller K O, McIntyre P B, Castello L, 2016. Balancing hydropower and biodiversity in the Amazon, Congo, and Mekong. *Science*, 351(6269): 128–129. doi: 10.1126/science.aac7082

Xia Jihong, Chen Yongming, Zhou Ziye et al., 2017. Review of mechanism and quantifying methods of river system connectivity. *Advances in Water Science*, 28(5): 780–787. (in Chinese)

Xia Zhijian, Bai Junhong, Jia Jia et al., 2015. Vertical distributions of contents and storage of carbon and nitrogen in soils in

Phragmite australis salt marshes in the Yellow River Delta. *Wetland Science*, 13(6): 702–707. (in Chinese)

Xu Guanglai, Xu Youpeng, Wang Liuyan, 2012. Evaluation of river network connectivity based on hydraulic resistance and graph theory. *Advances in Water Science*, 23(6): 776–781. (in Chinese)

Xu Li, Yu Guirui, He Nianpeng, 2019. Increased soil organic carbon storage in Chinese terrestrial ecosystems from the 1980s to the 2010s. *Journal of Geographical Sciences*, 29(1): 49–66. doi: 10.1007/s11442-019-1583-4

Yin Hongzhen, 2011. *Disentangling the Sources and Distribution of Sedimentary Organic Matters in the Yellow River Estuarine Wetlands Using Multi-tracer Approach*. Qingdao: Ocean University of China. (in Chinese)

Yu J B, Zhan C, Li Y Z et al., 2016. Distribution of carbon, nitrogen and phosphorus in coastal wetland soil related land use in the Modern Yellow River Delta. *Scientific Reports*, 6(1): 37940. doi: 10.1038/srep37940

Yu Junbao, Chen Xiaobing, Sun Zhigao et al., 2010. The spatial distribution characteristics of soil nutrients in new-born coastal wetland in the Yellow River Delta. *Acta Scientiae Circumstantiae*, 30(4): 855–861. (in Chinese)

Yu Junbao, Wang Yongli, Dong Hongfang et al., 2013. Estimation of soil organic carbon storage in coastal wetlands of modern Yellow River Delta based on landscape pattern. *Wetland Science*, 11(1): 1–6. (in Chinese)

Yu Zibo, Zhuang Tao, Bai Junhong et al., 2019. Seasonal dynamics of soil phosphorus contents and stocks in Suaeda salsa wetlands in the intertidal zone of the Yellow River Delta, China. *Journal of Agro-Environment Science*, 38(3): 633–640. (in Chinese)

Zhang Han, Ouyang Zhencheng, Zhao Xiaomin et al., 2018b. Effects of different land use types on soil organic carbon, nitrogen and ratio of carbon to nitrogen in the plow layer of farmland soil in Jiangxi Province. *Acta Scientiae Circumstantiae*, 38(6): 2486–2497. (in Chinese)

Zhang Mengmeng, Liu Mengyu, Chang Qingrui et al., 2018a. Spatial distribution of organic carbon in topsoil of the loess tableland in Shaanxi Province during 1985-2015. *Journal of Natural Resources*, 33(11): 2032–2045. (in Chinese)

Zhang Z S, Craft C B, Xue Z S et al., 2016b. Regulating effects of climate, net primary productivity, and nitrogen on carbon sequestration rates in temperate wetlands, Northeast China. *Ecological Indicators*, 70: 114–124. doi: 10.1016/j.ecolind.2016.05.041

Zhang Zhongsheng, Lü Xianguo, Xue Zhenshan et al., 2016a. Is there a redfield-type C:N:P ratio in Chinese wetland soils. *Acta Pedologica Sinica*, 53(5): 1160–1169. (in Chinese)

Zhang Zhongsheng, Yu Xiaojuan, Song Xiaolin et al., 2019. Impacts of hydrological connectivity on key ecological processes and functions in wetlands: a general review. *Wetland Science*, 17(1): 1–8. (in Chinese)

Zhao Q Q, Bai J H, Liu Q et al., 2016. Spatial and seasonal variations of soil carbon and nitrogen content and stock in a tidal salt marsh with *Tamarix chinensis*, China. *Wetlands*, 36(S1): 145–152. doi: 10.1007/s13157-015-0647-1

Zhao Q Q, Bai J H, Lu Q Q et al., 2017. Effects of salinity on dynamics of soil carbon in degraded coastal wetlands: implications on wetland restoration. *Physics and Chemistry of the Earth, Parts A/B/C*, 97: 12–18. doi: 10.1016/j.pce.2016.08.008

Zhao Q Q, Bai J H, Zhang G L et al., 2018. Effects of water and salinity regulation measures on soil carbon sequestration in coastal wetlands of the Yellow River Delta. *Geoderma*, 319: 219–229. doi: 10.1016/j.geoderma.2017.10.058

Zhu Fawen, Lu Zhihua, Cai Mei et al., 2017. Evaluation of river network connectivity in plain area of Taihu basin. *Hydro-Science and Engineering*, (4)52–58. (in Chinese)

Zou Yuxuan, Cheng Jing, Liu Kang et al., 2015. The contents of carbon and nitrogen of different forms and distribution of ammonia oxidizing prokaryotes in soils of ancient Yellow River. *Wetland Science*, 13(6): 752–758. (in Chinese)

Zuecco G, Rinderer M, Penna D et al., 2019. Quantification of subsurface hydrologic connectivity in four headwater catchments using graph theory. *Science of the Total Environment*, 646: 1265–1280. doi: 10.1016/j.scitotenv.2018.07.269